Helmholtz-Zentrum Dresden-Rossendorf (HZDR)

HELMHOLTZ ZENTRUM
DRESDEN ROSSENDORF

Positron Annihilation Studies using a Superconducting Electron LINAC

Wagner, A.; Butterling, M.; Hirschmann, E.; Krause-Rehberg, R.; Liedke, M. O.;
Potzger, K.;

Originally published:

May 2018

AIP Conference Proceedings 1970(2018), 040003

DOI: https://doi.org/10.1063/1.5040215

Perma-Link to Publication Repository of HZDR:

https://www.hzdr.de/publications/Publ-26064

Release of the secondary publication
on the basis of the German Copyright Law § 38 Section 4.

Positron Annihilation Lifetime and Doppler Broadening Spectroscopy at the ELBE Facility

Andreas Wagner[1, a)], Maik Butterling[1], Maciej O. Liedke[1], Kay Potzger[2], and Reinhard Krause-Rehberg[3]

[1]*Helmholtz-Zentrum Dresden-Rossendorf, Institute of Radiation Physics*
Bautzner Landstraße 400, 01328 Dresden, Germany
[2]*Helmholtz-Zentrum Dresden-Rossendorf, Institute of Ion Beam Physics and Materials Research*
Bautzner Landstraße 400, 01328 Dresden, Germany
[3]*Martin-Luther Universität Halle-Wittenberg, Institut für Physik, 06099 Halle, Germany*

[a)]Corresponding author: a.wagner@hzdr.de

Abstract. The Helmholtz-Zentrum Dresden-Rossendorf operates a superconducting linear accelerator for electrons with energies up to 35 MeV and average beam currents up to 1.6 mA with bunch charges up to 120 pC. The electron beam is employed to produce several secondary beams including X-rays from bremsstrahlung production, coherent IR light in a Free Electron Laser, superradiant THz radiation, neutrons, and positrons. The secondary positron beam after moderation feeds the Monoenergetic Positron Source (MePS) where positron annihilation lifetime (PALS) and positron annihilation Doppler-broadening experiments in materials science are performed. The adjustable repetition rate of the continuous-wave electron beams allows matching of the pulse separation to the positron lifetime in the sample under study. The energy of the positron beam can be set between 0.5 keV and 20 keV to perform depth resolved defect spectroscopy and porosity studies especially for thin films. Bulk materials, fluids, gases, and even radioactive samples can be studied at the unique Gamma-induced Positron Source (GiPS) where an intense bremsstrahlung source generates positrons directly inside the material under study. A ^{22}Na-based monoenergetic positron beam serves for offline experiments and additional depth-resolved Doppler-broadening studies complementing both accelerator-based sources.

INTRODUCTION

Positron annihilation lifetime spectroscopy (PALS) serves as a unique tool for the characterization of lattice defects in materials science. While the annihilation lifetime yields characteristic information about the size of open-volume defects ranging from single atomic vacancies up to even porous microstructures, the kinematical Doppler-broadening of annihilation radiation tells about the local electron momentum distribution at the annihilation site. Long annihilation lifetimes in the order of ns result from production of positronium, especially in porous media and in polymers. The well-established technique of employing radionuclides simultaneously emitting gamma-rays and positrons of typically up to several hundreds of keV is widely applied. Annihilation lifetimes are monotonously related to the void size with a surprisingly low dependence on the material surrounding the void [1]. The quantitative determination of positron annihilation lifetimes nevertheless is hampered when thin films or layered structures with sub-µm thicknesses which are of high technological relevance are considered. The isotropic emission and the high energy of common positron emitters cause penetration depths which are on the mm-scale. The installation described here overcomes this limitation by using mono-energetic positron beams with kinetic energies between 0.5 keV and 20 keV thus enabling depth-dependent thin film studies on the nm to µm scale [2].

THE MONOENERGETIC POSITRON SOURCE

The Mono-energetic Positron Source MePS has been set up at the superconducting electron linear accelerator ELBE (Electron LINAC with high Brilliance and low Emittance) [3] at Helmholtz-Zentrum Dresden-Rossendorf in a collaborative effort between Martin-Luther University Halle-Wittenberg and the Helmholtz-Zentrum Dresden-Rossendorf. Figure 1 shows the layout of the system schematically. Some of the details of the installation are described below.

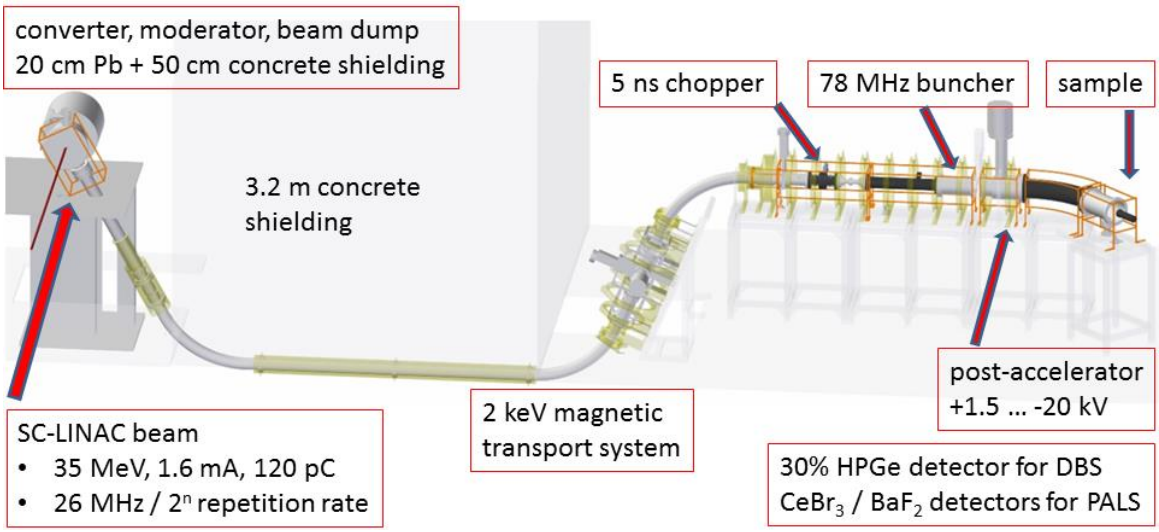

FIGURE 1: Layout of the Monoenergetic Positron Source at ELBE. DBS stands for Doppler-broadening Spectroscopy and PALS stands for Positron Annihilation Lifetime Spectroscopy.

The incident electron beam is delivered by the superconducting (SC) electron linear accelerator ELBE with energies up to 35 MeV. In contrast to conventional normal conductive accelerators superconducting technology makes possible the application of continuous radio-frequency accelerating electromagnetic fields with electric field gradients up to 20 MV/m. The injection of electrons from an injector can be done in principle with any divisor of the base frequency which is 1.3 GHz for ELBE. However, pulse-preforming by the electron beam bunching system prior to injection restricts the maximum applicable pulse repetition rate to 260 MHz. For positron annihilation studies repetition rates of 1.625 MHz, 6.5 MHz, 13 MHz, and 26 MHz have been employed up to now. The repetition rates have been selected in order to match to the annihilation lifetimes in the samples. Minimization of the effect of pulse-overlap (lower repetition rate favored) has been done while maximizing the detection efficiency (higher repetition rate favored) at given electron beam bunch charges. If we request a pulse-overlapping fraction of not more than one part in a 10^5, maximal annihilation lifetimes should be 54 ns, 14 ns, 7 ns, and 3 ns for the canonical repetition rates given above. The electron beam is directed towards a water-cooled tungsten bremsstrahlung converter consisting of 50 foils of 100 µm thickness each with a separation of 100 µm each as shown in figure 2, (a). The converter is enclosed in a stainless steel casing with attached stainless steel cooling pipes as shown in figure 2, (b). The converter has been designed to cope with average beam powers of up to 40 kW out of which only 4 kW have been used by now. Electron bremsstrahlung with a continuous spectrum up to the electron beam energy is then converted in turn by pair production into electrons and positrons inside the converter and also inside the following tungsten moderator.

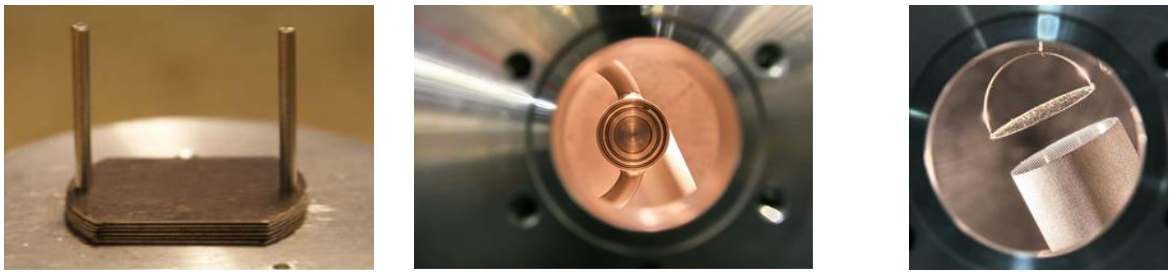

(a) (b) (c)

FIGURE 2: The bremsstrahlung converter and positron moderator. (a) Partially assembled stack of 50 Tungsten foils with 100 µm thickness each. (b) Assembled converter as viewed by the electron beam. (c) Moderator foil suspended above the accelerating grid at the entrance to an electrostatic lens.

Thermalized positrons from the moderator are being accelerated with a bias potential of +2 kV towards a conductive mesh at a few mm distance shown in figure 2, (c). Further positron transport is accomplished by a longitudinal magnetic field of 8 mT with variations of less than 10%. More than 3 m of iron-enriched concrete and 20 cm of lead shield the accessible laboratory from the positron generating converter. A water-cooled aluminium beam catcher of 600 mm length absorbs most of the radiation penetrating the converter and the moderator. Pure aluminium has been selected in order to minimize photo-neutron production owing the neutron separation energy of 13 MeV for ^{27}Al. The design of the beam catcher has been derived from the liquid lead photo-neutron source which is operated at ELBE [4].

After transporting the beam through the radiation shielding the beam is sent through a double beam chopper which imposes a transversal electric field of up to 500 V/cm, see figure 3, (a). The pulsed electric field has a Gaussian shape with a FWHM of 5 ns while the electrodes are separated by 6 mm. Out-of-phase positrons are deflected towards an adjustable aperture after half a gyration length of 126.3 mm. After removal of those non-phase matched positrons the beam is further longitudinally compressed with a double-slit buncher operating at a frequency of 78 MHz. A resonant circuit drives the central isolated drift tube while generating an electric field strength of up to 2.5 kV/cm at the two gaps, see figure 3, (b). The two buncher gaps are separated by 509 mm which matches to 3/2 times the buncher period at 2 keV positron transport energy.

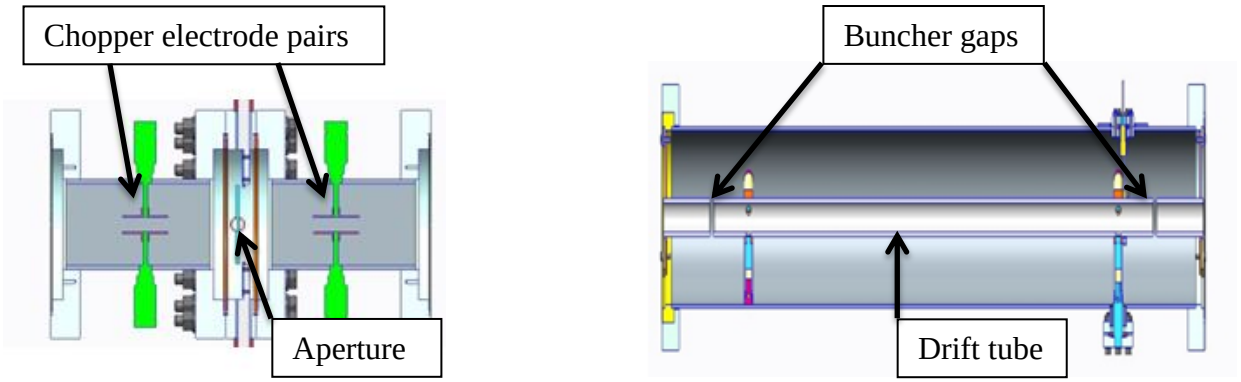

(a) (b)

FIGURE 3: (a) Beam chopper and (b) double-slit buncher. The beam enters from the left and additional beamline sections are omitted.

After longitudinal bunch compression by the chopper a 6-stage electrostatic acceleration structure follows which allows the positron kinetic energy and thus the penetration depth inside the sample to be varied. Prior to the target the magnetic guiding system is bent by 45° thus suppressing positrons reflected from the sample and bounced by the accelerator field to impact again onto the sample.

The sample station is kept at a potential of up to 25 kV. About 3 cm behind the sample a µ-metal shielded BaF_2 scintillation detector is employed for annihilation lifetime measurements. The detector has been recently substituted

by a $CeBr_3$ scintillation detector offering significant improvements with respect to disturbances from long scintillation lifetime components in BaF_2. The timing reference is derived from the precision master oscillator of the superconducting accelerator and is phase-matched to the electron bunches of the beam with a temporal jitter of 14 ps (FWHM). The signal-to-noise ratio is above 10^4 while lifetime resolutions of around 230 ps (FWHM) have been obtained. Figure 4 shows the positron annihilation lifetime of two reference samples with well-known annihilation lifetimes for an incident positron kinetic energy of 10 keV. On the left side, single crystalline Y_2O_3-stabilized ZrO_2 (YSZ) is shown together with a Gaussian distribution with a derived time resolution of 230 ps FWHM. On the right hand side, mono-crystalline silicon is shown. In both cases, the annihilation lifetimes of 181 ps and 218 ps, respectively, which were determined in conventional lifetime studies are well reproduced. Besides the main contribution an additional stable background lifetime of 720 ps of unknown origin is visible which is subtracted in all subsequent analysis. For both samples a signal to noise ratio of $5x10^5$ is obtained.

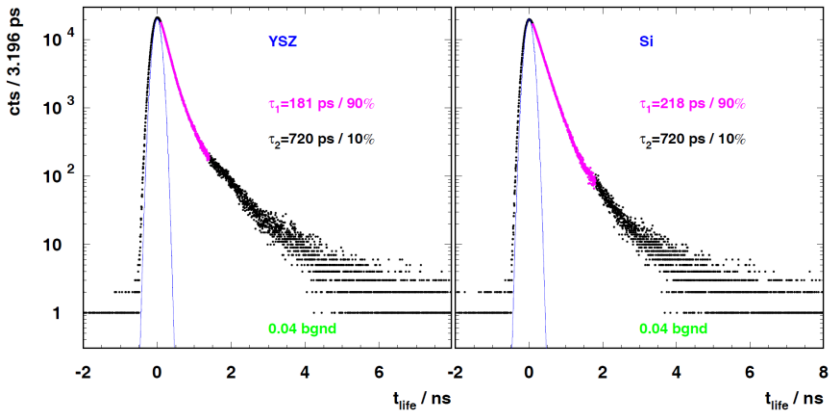

(a) (b)

FIGURE 4: Positron annihilation lifetime distributions for Y2O3-stabilized ZrO2 (a) and wafer-grade silicon (b). A Gaussian distribution with 230 ps FWHM (blue) is included in order to visualize the timing resolution.

An example for longer positron annihilation lifetimes is shown in figure 5, (a). It shows the variation of ortho-positronium lifetimes with the incident positron energies for nano-porous glasses. The µm-thin glass films have been produced by stimulated phase separation in sodium borosilicate glass into silica and an alkali borate phase thus generating sponge-like porous structures with unknown porosity [5]. Nano-porous glasses feature a tunable pore width and adjustable surface properties which makes them ideal candidates for separation membranes, chemo-sensors, drug delivery, optical coatings, and many other applications. Determination of porosity is hampered when employing conventional porosimetry methods. Both, Hg intrusion or LN2 sorption methods fail in the case of thin films due to weak signals from small surface areas and small porous volumes. Furthermore, systems with closed porosity cannot be investigated by means of intrusion techniques. In contrast, PALS serves as an ideal tool in such cases. Experimentally, the lifetime distributions are almost free from distortions and the peak to background ratios are between $5x10^4$ and $8x10^4$ due to a slight pulse-to-pulse overlap with the selected beam repetition rate of 1.625 MHz which corresponds to 615 ns pulse-to-pulse spacing.

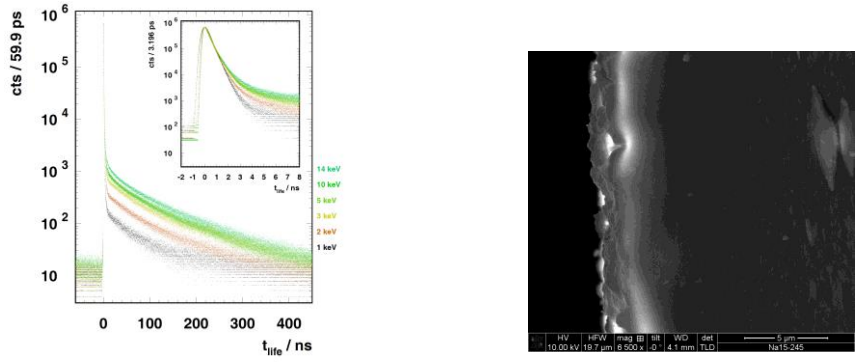

(a) (b)

FIGURE 5: (a) Positron annihilation lifetime distributions for nano-porous glasses (inset shown with increased time dispersion). (b) SEM picture of the nano-porous film with the surface on the right side and the non-porous structure extending from the center to the right side.

Due to imperfect bunching the timing resolution decreases for positron beam energies below 2 keV. The sample had been covered with a thin carbon layer to prevent positronium from escaping the surface. Figure 5, (b) shows a scanning electron microscope picture of a sample cut. The nano-porous film has a thickness of about 4 µm.

MePS has also been employed successfully for porosity studies of ultra low-k dielectric thin films as promising materials for advanced inter-connects scheme of ultra-large scale integrated devices. The aim is the reduction of resistance-capacitance delay and cross-talk noise by the introduction of nano-scale voids inside the insulating SiO_2 [6,7].

THE GAMMA-INDUCED POSITRON SOURCE

A second accelerator-driven positron source is realized in the so-called Gamma-induced Positron Source (GiPS) [8]. A pioneering technology called "accelerator-based γ-ray-induced PAS" or AGAPS at a normal conducting electron LINAC had been developed at Idaho State University and it was used for Doppler-broadening spectroscopy experiments [9]. The setup employs high-energy bremsstrahlung for pair production right inside the sample under study. The GiPS setup additionally allows annihilation lifetime experiments, as well, and it is especially suited for extended bulk samples, or samples which cannot be exposed to external positrons sources like positron beams or radioactive sources or because they are imposing hazardous conditions (high pressure, high temperature, intrinsic radioactivity), or if the sample handling imposes difficulties (fluids, gases, organic samples).

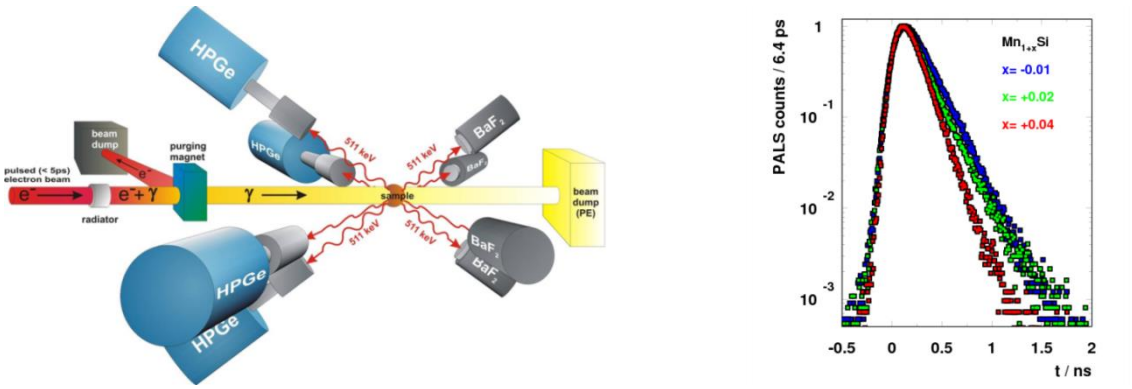

(a) (b)

FIGURE 6: (a) The Gamma-induced Positron Source at ELBE. Four identical pairs of High-Purity Germanium (HPGe) detectors for high energy resolution and BaF2 scintillation detectors for high timing resolutions are arranged around the sample. (b) Example of annihilation lifetime distributions (scaled) for three cases of slightly over- and under-stoichiometric contents of Mn in MnSi alloys.

Derived from a setup for nuclear resonance fluorescence studies [10] special emphasis has been put on background reduction and shielding. Recently, positron annihilation lifetime studies on point defects in the skyrmion-lattice compound MnSi [11] and on the origin of luminescence and scintillation in ZnO [12] have been published. Figure 6, (b) shows three annihilation lifetime distributions for slightly under- and over-stoichiometric Mn contents in MnSi alloys. For x<0, a single lifetime component of 185(4) ps agrees very well with the calculated lifetime of 181 ps for a single Mn vacancy in MnSi acting as a positron trap. For x>0, the lifetime distributions tend to become narrower while approaching the calculated bulk lifetime of 111 ps. Both features are in line with Coincidence Doppler-Broadening Spectroscopy results as discussed in [11].

As for the MePS source the beam repetition rate can be matched to the positron annihilation lifetime thus optimizing for high average intensity and low detector pile-up distortions.

THE SLOW POSITRON SYSTEM OF ROSSENDORF

While the accelerator-driven positron sources require sharing beam time with users of other beam lines, complementary Doppler-broadening spectroscopy studies are being performed at the ^{22}Na-based mono-energetic positron beam SPONSOR (Slow POsitroN System Of Rossendorf) [13]. The setup is shown in figure 7, (a). Here, Doppler-broadening studies are performed with higher statistics and more energy steps. Additionally, with both Germanium detectors arranged face-to-face and perpendicular to the beam line coincidence Doppler-broadening experiments are performed which allow for a two order of magnitude improvement in signal to noise ratio.

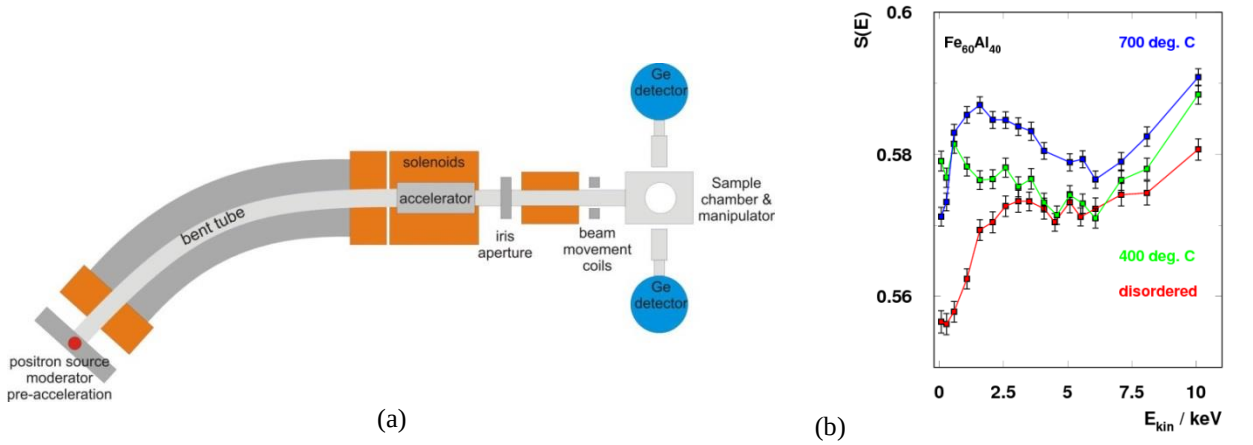

FIGURE 7: (a) The Slow Positron System at Rossendorf (SPONSOR). (b) Energy-dependent line-shape parameter variations for thin $Fe_{60}Al_{40}$ films after in-situ temperature treatments.

One of the main motivations for the additional setup is that it allows studying samples independently from available beam time at the main accelerator prior to measurements there. E.g., positron energy ranges for Positron Annihilation Lifetime experiments at MePS are determined using Doppler-broadening studies DBS at SPONSOR. Being a quite reliable and versatile stand-alone setup, many publications in various defect studies have successfully demonstrated the need for such a complementary setup. Most recently, post-growth treatment studies on defects in ALD-grown thin ZnO films [14] and the role of Zn vacancies in sol-gel prepared ZnO films [15] have been investigated. ^{22}Na-based lifetime experiments for bulk materials can be performed at a conventional lifetime setup.

THE APPARATUS FOR IN-SITU DEFECT ANALYSIS (AIDA)

In the future, MePS will be complemented by an ultra-high vacuum system for in-situ defect studies called Apparatus for In-Situ Defect Analysis (AIDA). Here, the introduction and the annealing of defects during ion-irradiation, temperature treatment and during thin film growth will be studied with a focus on novel energy-related materials. The AIDA system allows investigating of defects near the surface of a material, i.e. in an early stage of defect development, as well as in-situ "live" measurements. Currently, the interaction of such defective materials with hydrogen is investigated.

As a precursor for the MePS installation a pre-stage of AIDA has been implemented at the SPONSOR beam and in-situ experiments on the influence of defects on magnetic phase transitions in $Fe_{60}Al_{40}$ alloys [16] and on Cr_2O_3 which is used in a purely antiferromagnetic magneto-electric random access memory have been performed [17]. As an exemplary result figure 7, (b) shows the energy-dependent shape parameter variations for thin $Fe_{60}Al_{40}$ films after in-situ temperature treatments. The line-shape parameter *S* measures the ratio between those annihilation gamma-rays in a narrow energy region around 511 keV and all annihilation photons. Larger *S* parameters indicate larger molecular free volumes. Increase of S evidences an emerging ordered paramagnetic B2-phase containing vacancy complexes located in the Fe-sublattice as compared to the disordered A2-phase where randomly distributed mono-vacancies are expected. In addition, segregation of Al has been found for higher temperatures. The AIDA system (see figure 8) consists of an ultra-high vacuum system for annealing, metallic thin film deposition, and low-temperature ion irradiation. A four-point resistometry setup and an X-ray photoelectron spectroscopy (XPS) unit are optional characterization methods while maintaining vacuum conditions and temperature. Parts of the system are already installed at the 6 MV ion accelerator at HZDR where it is being used in Hydrogen-depth profiling studies employing the $^{1}H(^{15}N,\alpha\gamma)^{12}C$ reaction [19]. The positron beam transport system is currently under construction.

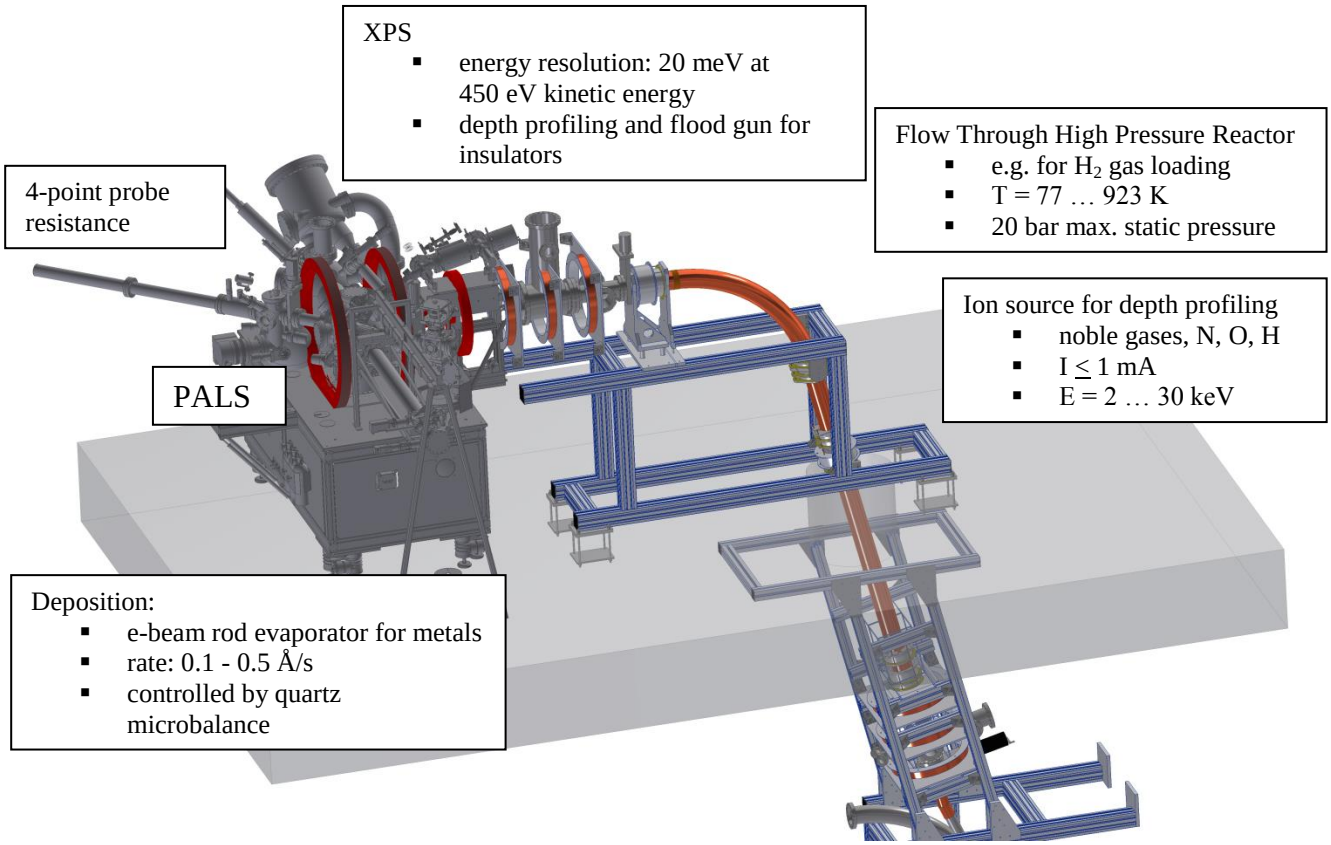

FIGURE 8: The Apparatus for In-situ Defect Analysis (AIDA) which is currently being set up on top of the monoenergetic positron beam MePS at ELBE.

CONCLUSIONS

The monoenergetic positron source MePS and the Gamma-induced Positron Source GiPS represent the first accelerator-based setups for positron annihilation lifetime, Doppler-broadening and age-momentum correlation measurements operated at a superconducting RF accelerator in a continuous wave mode. Adjustable beam repetition rates are selected to match annihilation lifetimes in order to obtain efficient measurements and low pile-up distortions. Conventional positron sources complement the accelerator-based setups for in-depth and precursor studies. Positron annihilation lifetime and Doppler-broadening experiments are complemented by new facilities for defect analysis during in-situ material modifications and thin film growth.

ACKNOWLEDGEMENTS

The pre-stage system of AIDA was funded by the Initiative and Networking Fund of the Helmholtz-Association. (FKZ VH-VI-442 Memriox). Thanks go to the ELBE accelerator crew for providing stable beams, to M. Görler, A. Hartmann, A. Müller, D. Stach, and G. Staats for their contributions to the beam transport, buncher and chopper system, and especially to M. Jungmann for his invaluable contributions to the MePS setup.

REFERENCES

1. K. Wada and T. Hyodo, Journal of Physics: Conf. Series **443**, 012003 (2013).
2. R. Krause-Rehberg, G. Brauer, M. Jungmann, A. Krille, A. Rogov, K. Noack, Appl. Surf. Sci. **255,** 22 (2008).
3. F. Gabriel, P. Gippner, E. Grosse, D. Janssen, P. Michel, H. Prade, A. Schamlott, W. Seidel, A. Wolf, R. Wünsch, Nuclear Instruments and Methods in Physics Research B **161**, 1143 (2000).
4. E. Altstadt, C. Beckert, H. Freiesleben, V. Galindo, E. Grosse, A. R. Junghans, J. Klug, B. Naumann, S. Schneider, R. Schlenk, A. Wagner. F.-P. Weiss, Annals of Nuclear Energy **34**, 36 (2007).
5. H. Uhlig, G. Adouane, C. Bluhm, S. Zieger, R. Krause-Rehberg, D. Enke, Journal of Porous Materials **23**, 139 (2016).
6. M. Jungmann, J. Haeberle, R. Krause-Rehberg, W. Anwand, M. Butterling, A. Wagner, J. M. Johnson, T. E. Cowan, Journal of Physics: Conference Series **443**, 012088 (2013)
7. A. Uedono, S. Armini, Yu. Zhang, T. Kakizaki, R. Krause-Rehberg, W. Anwand, A. Wagner, Applied Surface Science **368**, 272 (2016)
8. M. Butterling, W. Anwand, T. E. Cowan, A. Hartmann, M. Jungmann, R. Krause-Rehberg, A. Krille, A. Wagner, Nuclear Instruments and Methods in Physics Research B **269**, 2623 (2011).
9. F. A. Selim, D. P. Wells, J. F. Harmon, J. Williams, Journal of Applied Physics **97**, 113539 (2005)
10. R. Schwengner, R. Beyer, F. Dönau, E. Grosse, A. Hartmann, A. R. Junghans, S. Mallion, G. Rusev, K.-D. Schilling, W. Schulze, A. Wagner, Nuclear Instruments and Methods in Physics Research A **555**, 211 (2005).
11. M. Reiner, A. Bauer, M. Leitner, T. Gigl, W. Anwand, M. Butterling, A. Wagner, P. Kudejova, C. Pfleiderer, C. Hugenschmidt, Scientific Reports **6**, 29109 (2016).
12. J. Ji, A. M. Colosimo, W. Anwand, L. A. Boatner, A. Wagner, P. S. Stepanov, T. T. Trinh, M- O. Liedke, R. Krause-Rehberg, T. E. Cowan, F. A. Selim, Scientific Reports **6**, 31238 (2016).
13. W. Anwand, G. Brauer, M. Butterling, H. R. Kissener, A. Wagner, Defect and Diffusion Forum **331**, 25 (2012).
14. M. Haseman, P. Saadatkia, D. J. Winarski, F. A. Selim, K. D. Leedy, S. Tetlak, D. C. Look, W. Anwand, A. Wagner, Journal of Electronic Materials **45**, 6337 (2016).
15. D. J. Winarski, W. Anwand, A. Wagner, P. Saadatkia, F. A. Selim, M. Allen, B. Wenner, K. Leedy, J. Allen, S. Tetlak, D. C. Look, AIP Advances **6**, 095004 (2016).
16. M. O. Liedke, W. Anwand, R. Bali, S. Cornelius, M. Butterling, T. T. Trinh, A. Wagner, Journal of Applied Physics **117** 163908 (2015).
17. T. Kosub, M. Kopte, R. Hühne, P. Appel, B. Shields, P. Maletinsky, R. Hübner, M. O. Liedke, J. Fassbender, O. G. Schmidt, D. Makarov, Nature Communications **8**, 13985 (2017).
18. J. Čížek, F. Lukáč, I. Procházka, R. Kužel, Y. Jirásková, D. Janičkovič, W. Anwand, G. Brauer, Physica B **407**, 2659 (2012).
19. T. P. Reinhardt, S. Akhmadaliev, D. Bemmerer, K. Stöckel, L. Wagner, Nuclear Instruments and Methods in Physics Research B **381**, 58(2016).